We are IntechOpen,
the world's leading publisher of
Open Access books
Built by scientists, for scientists

6,900
Open access books available

185,000
International authors and editors

200M
Downloads

Our authors are among the

154
Countries delivered to

TOP 1%
most cited scientists

12.2%
Contributors from top 500 universities

BOOK CITATION INDEX
CLARIVATE ANALYTICS
INDEXED

WEB OF SCIENCE™

Selection of our books indexed in the Book Citation Index
in Web of Science™ Core Collection (BKCI)

Interested in publishing with us?
Contact book.department@intechopen.com

Electrodeposition of Alloys Coatings from Electrolytic Baths Prepared by Recovery of Exhausted Batteries for Corrosion Protection

Paulo S. da Silva, Jose M. Maciel, Karen Wohnrath,
Almir Spinelli and Jarem R. Garcia

Additional information is available at the end of the chapter

1. Introduction

Electrical and electronic equipment have developed rapidly and their average life spans have been reduced due to the changes in functions and designs [1-3]. Recently, the recovery of precious metals from these electronic scraps has become attractive. Precious metals and copper in PC board scraps and waste mobile phones account for more than 95% of the total intrinsic value [4] and recently several authors are carrying out study on the applicability of economically feasible hydrometallurgical processing routes to recover precious metals [3-5].

Due to this massive industrialization of electronic equipment like toys, cameras, laptops, cell phones, etc [6]. In recent years there has been a considerable increase in the consumption of household batteries The American industry invoice approximately 2.5 billion dollars annually selling about 3 billion batteries. In Europe in the year of 2003 were produced 160,000 tonnes of portable batteries. In this year in Brazil the annual production of these devices reaches about 1 billion units [7, 8]. In this way spent batteries represent an increasing environmental problem due to the high content of heavy metals. Unlike large batteries used for vehicles, small, portable batteries are very diverse in terms of chemical composition and represent 80–90% of all portable batteries collected [9, 10]. The difference between various types of used battery is represented by the used materials such as electrolytes and electrodes [9]. These batteries can be sorted by size, shape and chemical composition so that we can determine which metals can be recovered from each category.

For these reasons in several countries, collecting batteries is becoming mandatory, and so is recycling those containing toxic materials. Recycling may also be applied to recovering valuable materials to be reutilized [11].

There are basically two types of household batteries: primary batteries that after becoming worn are discarded and the secondary batteries that can be recharged [12, 13]. Within the wide range of commercially available batteries zinc-carbon batteries (also known as Leclenché or dry cells) and alkaline batteries are the most consumed because of its low cost. In Europe, from the total of batteries sold in 2003, 30.5% and 60.3%, were Zn-C batteries and alkaline batteries, respectively. In China are produced annually more than 15 billion of these devices and in Brazil estimating a consumption of six batteries per inhabitant per year [7, 8, 14].

The disposal of these batteries is a serious problem, because in their composition there are metals considered dangerous to the environment [13]. The cost for the safe disposal of these materials is quite high due to the large amount of dangerous waste generated and due to the fact that the storage capacity in landfills or dumps is running out. A policy adopted in 2006 by the European Union (EU) banned incineration and disposal of batteries in landfills. This regulation applies to all types of batteries regardless of shape, volume, weight, composition or use. Through this new policy it is expected to mobilize the EU countries member for the collection, recovery and recycling of metals present in these power devices [15]. In Brazil, according to the resolution 401/2008 of the *Brazilian National Council of the Environment* (CONAMA in Portuguese) [16], after consumption, household batteries must be collected and sent to the manufacturers, to be recycled, treated or disposed of an environmentally safe way, but until 1999 they could be disposed of in household waste since meet the limits of heavy metals in its composition. Although required, this resolution proved to be insufficient to solve the problem of environmental contamination by means of this waste since there is a large annual consumption of these batteries. A factor to be noted is that in spite of Zn and Mn match most of the composition of cells $Zn-MnO_2$, the limits of contamination of these metals are not established by law. Another aggravating factor is the use of irregular cells entering the Brazilian market. Frequently these products do not meet manufacturing standards. The heavy metal content of these cells is seven times greater than that limited established by the CONAMA. Thus, the contamination starts by improper disposal of these devices in landfills or dumps, which is the destination of the majority of household solid waste in Brazil [13,16, 17].

Industrial recycling of batteries is generally focused on two processes: the pyrometallurgical and/or the hydrometallurgical. The pyrometallurgical method is based on the difference of volatilization of different metals at high temperatures followed by condensation. The hydrometallurgical method is based on the dissolution of metals in acidic or alkaline solutions. The advantage of the first method is the absence of the necessity of dismantlement of the devices. However, it is an expensive process, since it requires high temperatures and is not efficient selectively, for example, to obtain pure zinc from $Zn-MnO_2$ batteries, Ni-Cd batteries cannot be treated simultaneously because the Zn and Cd are not selectively volatized in the oven, so sorting steps are required in advance of the materials recycling. Another drawback is related to the production of dust and gas emission into the atmosphere during the recycling process. The hydrometallurgical route is usually more economical and efficient than the pyrometal-

lurgical process. In addition there is a diminishment of the emission of particles into the atmosphere. However, it is a more laborious process requiring pretreatment steps such as sorting, disassembling and leaching of material to improve the dissolution of metals in aqueous phase. In addition, the recovery of metals requires different aqueous media (acid or alkaline) and various processes of precipitation [14, 18, 19].
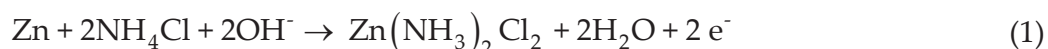
The recovery of these materials is very important because in addition to reducing the enormous amount of waste generated by consume of these power devices, recycling could lower the cost of production of new batteries through the reuse of raw materials by recycling and, conse-quently it reduces the risks to the environment [19, 20].

2. Features of Zn-MnO$_2$ batteries

Zn-C (also known as Leclanché or Zn-MnO$_2$ Batteries) batteries and alkaline batteries are basically composed by potassium, manganese and zinc as metal species. The stack of Zn-C was invented in 1860 by George Leclanché and the devices currently used are very similar to the original version.

A schematic view of this type of batteries is showed in Figure 1. In these batteries the anode consists of a zinc metal cylinder used, usually in the form of plate to procedure the outside structure of the cell. The cathode consists of a graphite rod surrounded by a powder mixture of graphite and manganese dioxide. The electrolyte is a mixture of ammonium chloride and zinc chloride. During the Zn-C and alkaline batteries discharge, basically the following reactions are observed:
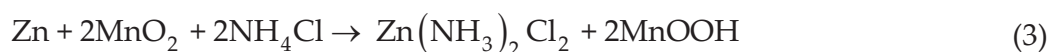
Zinc oxidation at anode:

$$Zn + 2NH_4Cl + 2OH^- \rightarrow Zn(NH_3)_2 Cl_2 + 2H_2O + 2\ e^- \tag{1}$$

Manganese reduction at cathode:

$$2MnO_2 + 2H_2O + 2e^- \rightarrow 2OH^- + 2MnOOH \tag{2}$$

Resulting in the overall reaction:

$$Zn + 2MnO_2 + 2NH_4Cl \rightarrow Zn(NH_3)_2 Cl_2 + 2MnOOH \tag{3}$$

In this kind of batteries, during storage and in rest periods while operating some parallel reactions can occur, causing leaks and loss of efficiency. In this way, some metals such as Cd,
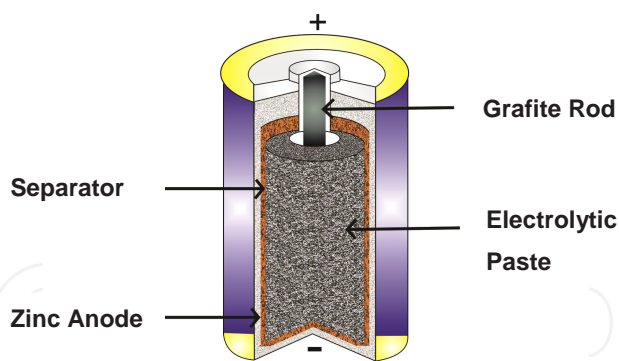
Figure 1. Schematic View of the Zn-MnO$_2$ Battery (Leclanché Device)

Cr, Hg and Pb are added to these devices to improve their performance and to avoid these parallel reactions.

The alkaline battery is a modified version of the stack of Zn-C. It features the same electrodes (anode and cathode), however, the electrolyte is a concentrated potassium hydroxide folder containing zinc oxide. Another difference is that its outer part is made on steel plate for assuring better seal. The reactions that occur in the cathode during discharge are the same that occurs in the Zn-C batteries, but the anodic reactions are different:

Zinc oxidation at alkaline batteries anode:

$$Zn + 2OH^- \rightarrow Zn(OH)_2 + 2e^-$$ (4)

Resulting in the overall reaction:

$$Zn + 2MnO_2 + 2H_2O \rightarrow Zn(OH)_2 + 2MnOOH$$ (5)
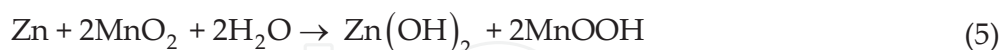
The advantage of the alkaline batteries is that they do not have parallel reactions and can be stored for up to four years keeping more than 80% of their original capacity, additionally its lifetime is up to ten times higher, however they are on average five times more expensive. Alkaline batteries are placed on the market as "mercury-free", however the literature reports that in several works on recycling of batteries were found heavy metals in these devices, including mercury [19-23]. The composition of some alkaline batteries and Zn-C are given in Table 1.

These portable batteries (alkaline and Zn–C) contain Mn and Zn in high concentrations. Considering that the production of these kind of power device are increasing it has become important the usage of recycled metals production instead of primary metals. Besides the positive impact on the environment, in the recuperation process of materials lot of energy is

Metal	A1[a] % in weight*	A2[b] % in weight*	B1[c] % in weight*	B2[d] % in weight*
Zn	21	20,56	5	5,05
Mn	45	26,60	23-30	29,04
Fe	0,36	0,15	0,2-10	0,18
Hg	1 (ppm)	0,0012	-	-
Cd	0,06(ppm)	0,0007	-	0,0002
Pb	0,03	0,005	-	-
Ni	-	0,008	0,007	0,006
K	4,7	7,3	-	-

* (% in weight of the electrolytic paste)

[a]Alkaline [23]; [b]Alkaline [22]; [c]Zn-C [23] and [d]Zn-C [21].

Table 1. Composition of $Zn-MnO_2$ and Alkaline Cells.

saved and the pollution is also reduced as the chemical treatment of primary metals is not needed. Manganese and zinc are important metals in many fields. Zinc is the most important nonferrous metal after copper and aluminum [23] and of the total zinc consumption, 55% is used to cover other metals to prevent oxidation, 21% in zinc-based alloys, 16% in brass and bronze. The increase of zinc demand in 2010 was due to a revival of the consumption in Europe (24%) and also to the consolidated economic growth of the emerging economies like Brazil, India and most notably China where the consumption increased 11% respect to 2009. Most of consumption of manganese is related to steel production, directly in pig iron manufacture and in the ferroalloy industry. Manganese resources are large but irregularly widespread in the world and South Africa and Ukraine account for about 75% and 10 % of the word´s identified manganese resources respectively [24].

Due to the growing interest in global environmental issues, recycling of Zn–Mn batteries carried more attentions and was reviewed in detail recently [15]. As the most widely used hydrometallurgical process, acid leaching was frequently used to release both Zn and Mn from the spent Zn–Mn batteries in the presence of strong acid solution such as H_2SO_4, HCl, HNO_3 and so on. In most cases, acid leaching produce nearly 100% of Zn extraction from the spent batteries, but Mn dissolution was rather poor due to insoluble MnO_2; moreover, the heavy consumption of various strong acids endowed the leaching process with high cost, strict requirements of equipment and potentially safe risk. The reductive acidic leaching could greatly improve extraction yield of Mn by adding inorganic reductants such as H_2O_2 and SO_2 or organic ones such as glucose, sucrose, lactose, oxalic acid, citric acid, tartaric acid, formic acid and triethanolamine, but higher safety risk and greater operation cost occurred [15]. So, developing the environmentally-friendly and cost-effective recycling methods for the spent Zn–Mn batteries are encouraged. At present, biohydrometallurgical processes (bioleaching-

tech) have been gradually replacing hydrometallurgical ones due to their higher efficiency, lower cost and few industrial requirements [25]. Bioleaching was characterized by efficient release of metals from solid phase into aqueous solution under the mild conditions of room temperature and pressure by contact and/or non-contact mechanisms in the presence of acidophilic sulfur-oxidizing and/or iron-oxidizing bacteria [26, 27].

Another alternative method developed for Zn-Mn batteries recycling is the electrodeposition of Zn and Zn–Mn alloy coatings over different kinds of steel to corrosion protection [28, 29]. Electrodeposited coatings of zinc are extensively employed in the protection of steel against corrosion. However, this protective effect is not very effective under aggressive atmospheric conditions [30]. In recent years, several materials have been investigated to improve the durability of these coatings. Electrodeposited alloys of Zn, such as Zn–Ni, Zn–Co and Zn–Fe, present higher corrosion resistance than pure zinc coatings. Also, it has been reported in the literature that Zn–Mn alloys show even better corrosion resistance properties [31–34]. The high corrosion resistance of these alloys is likely due to the dual protective effect of manganese: on the one hand Mn dissolves first because it is thermodynamically less noble than Zn, thereby protecting Zn; and on the other hand Mn ensures the formation of compounds with a low solubility product over the galvanic coating. Depending on the aggressivity of the environment to which the Zn–Mn alloy is exposed, various compounds may be found in the passive layer, including oxides such as MnO, MnO_2, Mn_5O_8 and γ–Mn_2O_3, or basic salts like $Zn_4(OH)_6SO_4.xH_2O$ and $Zn_5(OH)_8Cl.2H_2O$ [31, 35, 36]. The protective effect of Zn–Mn is dependent on the Mn content of the alloy. Although it has been reported that among the Zn alloys those of Zn–Mn show the highest corrosion resistance, their deposition process presents some drawbacks related to the bath instability and current efficiency. Among the various electrolytic baths and additives proposed to obtain Zn–Mn alloys, the use of a chloride-based acid bath with polyethylene glycol (PEG) as the additive seems very promising [31–33].

The mainly practical application in produce a protective Zn-Mn layer over steel is related to the substitution of the primary painting process on metallic parts produced in foundries. Furthermore it is important to note that beside the great interest in recycling Zn-C batteries the use solution produced by the acidic leaching of these exhausted batteries to obtaining protective Zn-Mn films were described only in two papers[28,29].

Considering the concepts described above this chapter brings some highlighting on the development of a methodology to recover zinc and manganese present in exhausted zinc–carbon batteries through chloride acidic leaching of the solid material. The leaching solution is then used as an electrolytic bath for the electrodeposition of the galvanic coating on AISI 1018 steel. Polyethylene glycol is used as the additive in the bath to obtain both Zn and Zn–Mn alloys.

3. Electrodeposition of Zn and Zn–Mn alloy coatings

To carrying out the electrodeposition of Zn and Zn–Mn Alloy coatings from electrolytic baths obtained from leaching of spent batteries is important to know the metallic composition and

concentration of the solution. Table 2 shows the typical composition obtained by an acid leaching with diluted HCl, of the carbon paste obtained from Zn-C spent batteries manufactured in Brazil [28]. This quantitative analysis of the metal content was performed by atomic absorption spectrometry and indicated that in addition to Zn^{2+} and Mn^{2+} traces of other species such as Fe^{2+}, Cu^{2+} and Pb^{2+} were present in solution.

Metal	Concentration (mg L^{-1})	Metal	Concentration (mg L^{-1})
Zn	6,981.33	Pb	55
Mn	3,030.30	Cr	0
Cu	30.4	Ag	0
Fe	5.5	Ni	0

Table 2. Composition of the Electrolytic Bath Obtained from Recycling of Zn-C Batteries.

It could be seen from the Table above that the batteries used containing Pb as heavy metal in their composition, however this quantity found corresponds to 0.18% by weight of the battery electrolytic paste that was in agreement with the limits established by CONOMA (0.20%).

To prepare the electrolytic bath from this solution the pH is adjusted to 5.0. During this step occurs the hydrolysis of some metallic ions forming a gelatinous brown material, possibly due to the formation of iron hydroxide that was removed by filtration. From this filtrated solution it was prepared four electrolytic baths used in obtaining the Zn-Mn alloy coatings. These baths were prepared to the addition of boric acid and different quantities of additives (ammonium isocyanate - NH$_4$SCN and polyethylene glycol – PEG$_{10.000}$) as showed in Table 3.

Bath Name	Zn	Mn	PEG$_{10.000}$	NH$_4$SCN	H$_3$BO$_3$
S$_0$			-	-	
S$_1$	0.10 mol L^{-1}	0.06 mol L^{-1}	1 g L^{-1}	-	0.32 mol L^{-1}
S$_2$			-	6.5 mmol L^{-1}	
S$_3$			1 g L^{-1}	6.5 mmol L^{-1}	

Table 3. Composition of the Obtained Electrolytic Bath through Recycling of Cells Used to Obtain Mn-Zn Alloys.

The behavior of AISI 1018 carbon steel electrodes in the presence of the electrolytic baths prepared from recycled batteries could be investigated by measurements of cyclic voltammetry. The Figure 2 shows the voltammetric curves obtained on 1018 carbon steel immersed in the proposed electrolytic baths (see Table 3). It could be seen from Figure 2a that with no additive on the bath the voltammogram showed two regions of reduction. The first region present a peak current with maximum current in -1.4 V and is related to the electrodeposition of zinc on the electrode. The second region present a continuous increase on reduction current starting on E = -1.5 V, this region can be related to the formation of Mn-Zn alloy, but tis increase

in cathodic current has an important contribution of the process of hydrogen evolution. This former observation is the reason of the needing of usage of additives that could be a hindrance for this reaction on the surface. When the potential is swept in the positive direction no peak of current is observed, just a constant increase on anodic current starting in almost E = -1.2 V, this current increase is related to the dissolution of metal layer deposited on the steel during the cathodic scan.
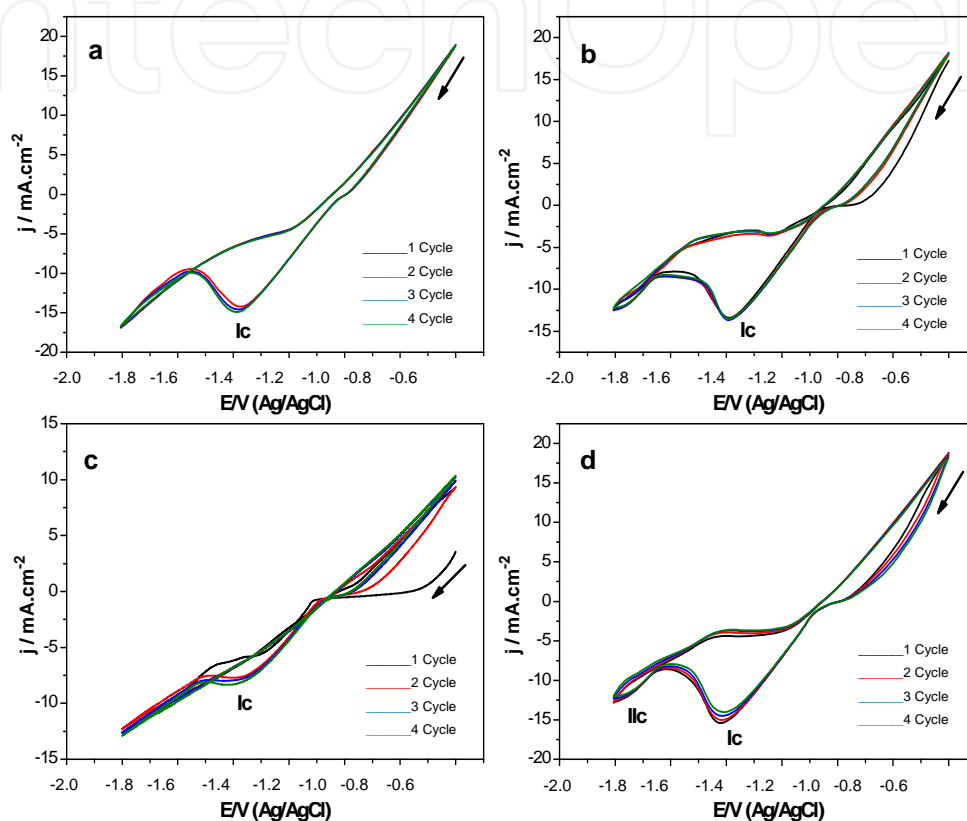

Figure 2. Voltammetric Curves Obtained on 1018 Carbon Steel Immersed in the Proposed Electrolytic Baths (see Table 3) (a) S0, (b) S1, (c) S2 and (d) S3 with scan rate = 20 mV s^{-1}.

No significant changes are observed with the addition of the addictive PEG$_{10,000}$ and with the addition of a mixture of NH$_4$SCN and PEG$_{10,000}$ (see Figures 2b and 2d), except by a slight diminishment on the current density, this loss in current density could be assigned to the presence of the additives. As discussed by Diaz-Arista et al. [31] the PEG$_{10,000}$ can adsorb on the steel surface blocking of the active sites for hydrogen evolution, but the isocyanate, according to these authors has the function of complexing with the ions Zn^{2+} decreasing the competition with the reduction of ions Mn^{2+}. However, in the presence of NH$_4$SCN the voltammetric curves are considerably different from the others conditions, as could be seen in Figure 2c. This figure shows that the process of Zn^{2+} electrodeposition, that occurred with a peak current at ca. -1.4 V in the other conditions, is now linked to the Mn^{2+} electrodeposition process as could be observed by the continuous increase in the cathodic current with the augment of the potential forward negatives values. This behavior was assigned to the fact that

the NH_4SCN has complex interactions with Zn^{2+} and Mn^{2+} decreasing the difference between the reduction potential of these two metallic species on the steel surface. The characterization of the coatings obtained with NH_4SCN as addictive showed films with bad quality as weak adherence to the surface, inhomogeneity, and with no increase in the Mn proportion related to the presence of Zn. For this reason this additive was not used in the others experiments described in this text.

After determining the potential range for reduction of the metallic ions Zn^{2+} and Mn^{2+} presented in the prepared electrolytic baths, the coating were obtained in the potentiostatic mode in two situations: first by application of -1.2 V and the second by application of -1.6 V during 15 min. The conditions used during the potentiostatic electrodeposition using the S0 and S1 solutions were chosen in agreement with previous studies carried out by other authors on the electrodeposition of Zn–Mn alloys [31]. The resulting current–time curves are shown in Figure 3. At -1.2 V, in the absence of additive, the current density stabilized at around -4.5 mA cm^{-2}. In the presence of PEG, the current density is slightly less negative (-3.6 mA cm^{-2}). When electrodeposition was carried out at -1.6 V the current densities with and without the additive were -17.6 mA cm^{-2} and -10.8 mA cm^{-2}, respectively. It is important to note that the presence of additive during the electrodeposition at more negative potentials makes the current density more stable. The instability observed in the electrodepositions carried out with S0 solution, particularly at -1.6 V, may be attributed to hydrogen evolution. In a study on the effect of additives on the hydrogen evolution reaction during Zn electrodeposition, Song et al. [37] suggested that PEG acts as an inhibitor of hydrogen absorption in the electrodeposited Zn.
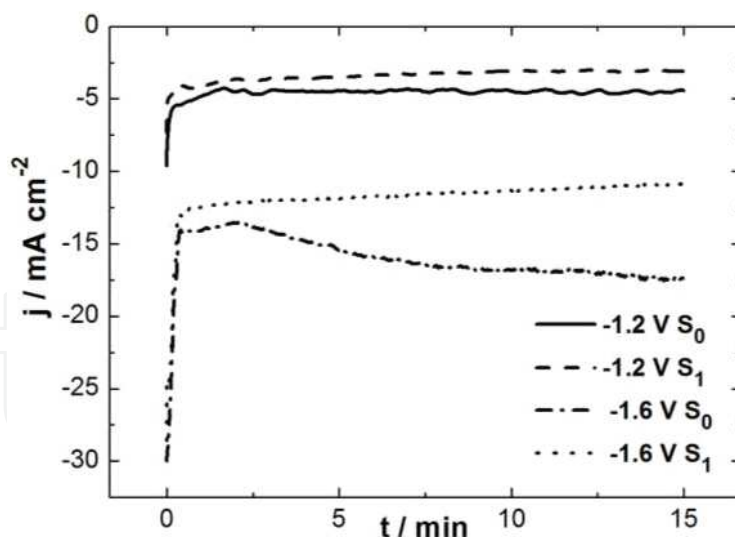

Figure 3. Potentiostatic curves obtained during electrodeposition onto an AISI 1018 steel electrode from S0 and S1 baths.

The characterization of the coating obtained potentiostatically was performed by measurements of Scan Electronic Microscopy (SEM), Energy Dispersion Spectroscopy (EDS) and X Ray Diffraction (XRD). The Figure 4 shows the morphology of the deposit obtained potentiostatically at -1.2 V from the base solution (S0). The SEM image shows that the deposit is comprised

of hexagonal plates with pyramidal clusters grouped into nodules of several sizes, as is normal for pure zinc electrodeposits [37]. The EDS analysis (inset on Figure 4) showed the presence of zinc as the predominant element in the coating.

In the presence of PEG, the deposit obtained is comprised of hexagonal crystals oriented perpendicularly to the substrate surface (Figure 5) and the zinc also was the predominant element (inset on Figure 5). This type of morphology was also observed by Ballesteros *et al.* [30] who studied the influence of PEG as an additive on the mechanism of Zn deposition and nucleation.
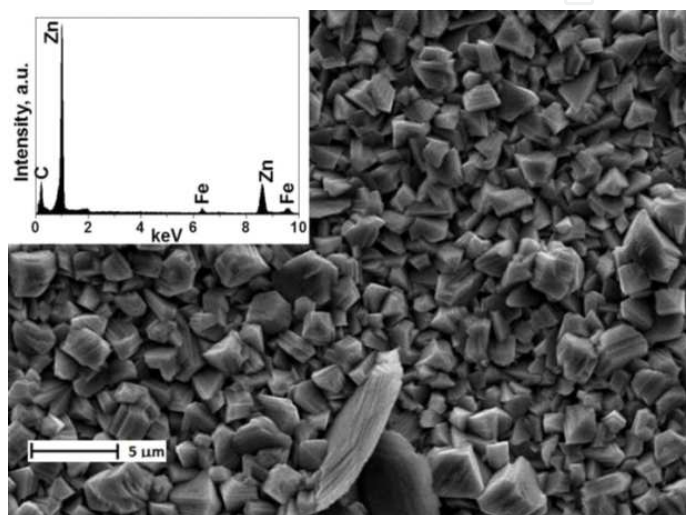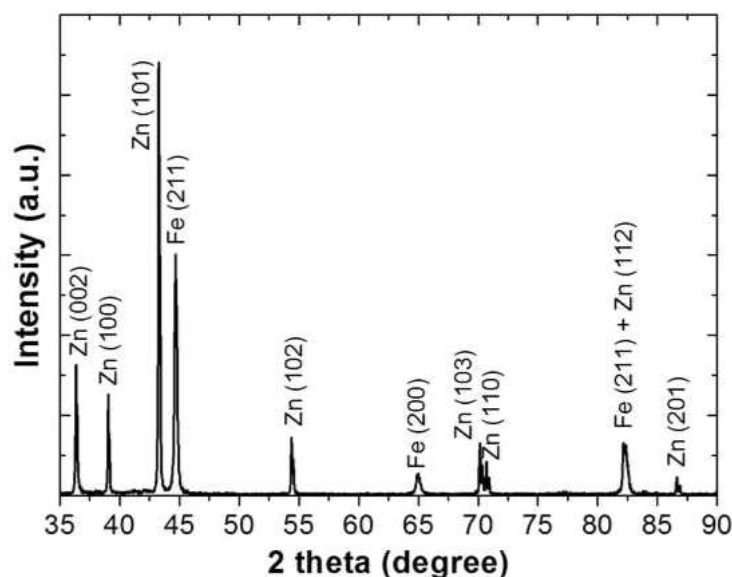

Figure 4. SEM image of the deposit formed on AISI 1018 steel electrode at -1.2V vs. (Ag/AgCl), polarization time = 15 min, using solution S0 as electrolytic bath. The results for the EDS analysis of the film are shown in the inset.
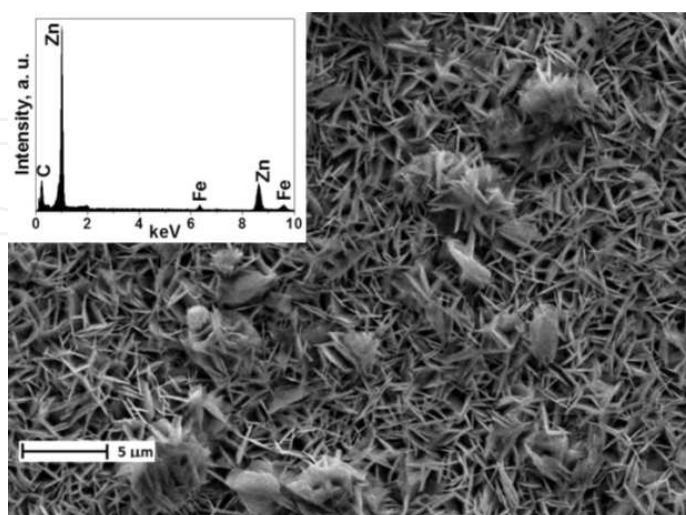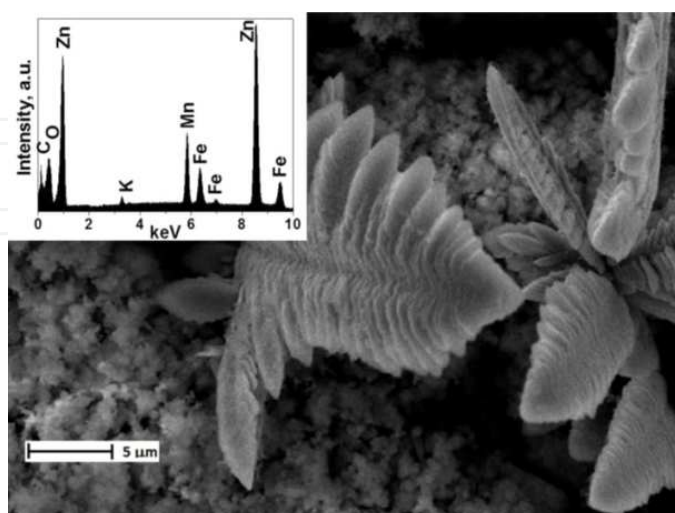

Figure 5. SEM image of the deposit formed on AISI 1018 steel electrode at -1.2V vs. (Ag/AgCl), polarization time = 15 min, using solution S1 as electrolytic bath. The results for the EDS analysis of the film are shown in the inset.

Although differences were observed in the morphology of the deposited coatings obtained with and without the use of the additive, the XRD analysis exhibited in Figure 6 showed the characteristics diffraction peaks for the coating obtained on AISI 1018 steel electrode at −1.2 V vs. (Ag/AgCl), t = 15 min, using the solution S0 (without additive). A similar composition was obtained with the bath S1 in the same electrodeposition condition. As can be seen, the formation of a Zn-Mn alloy could not be obtained from this potentiostatic experiments carried out at -1.2 V.
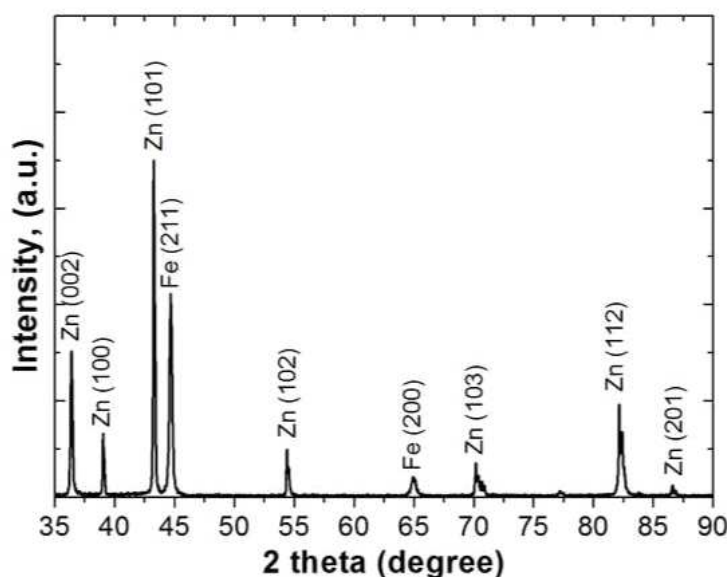

Figure 6. X-ray diffraction (XRD) pattern of the deposit obtained on AISI 1018 steel electrode at −1.2 V vs. (Ag/AgCl), t = 15 min.using the solution S0 (without additive).

Figure 7. SEM image of the deposit formed on AISI 1018 steel electrode at −1.6 V vs. (Ag/AgCl), t = 15 min, from solution S0. The results for the EDS analysis are shown in the inset.

Figure 7 shows the morphology of the deposit obtained potentiostatically at -1.6 V without the use of the additive. In the SEM image an amorphous and porous deposit covering some parts of the substrate can be observed. The EDS analysis (inset on Figure 7) indicated that the manganese content of this deposit is around 8% wt.

The XRD analysis of the coating obtained at −1.6 V vs. (Ag/AgCl) from solution S0 is showed in Figure 8. This XDR measurement also indicated that these experimental conditions did not favor the formation of a Zn-Mn alloy. This result may be related to the formation of $Mn(OH)_2(s)$ species on the substrate surface due to the hydrogen formation under these experimental conditions, resulting in an increase in the pH in the vicinity of the working electrode [38]. In addition, the formation of $Mn(OH)_2$ in high alkaline conditions agrees well with the Eh x pH (Pourbaix) diagrams [39].
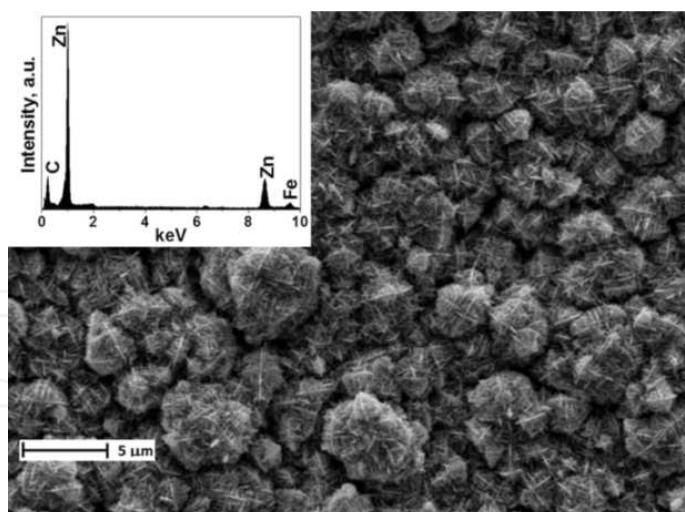

Figure 8. X-ray diffraction (XRD) pattern of the deposit obtained on AISI 1018 steel electrode at −1.6 V vs. (Ag/AgCl), t = 15 min.using the solution S0 (without additive).

In comparison with the morphology observed for the deposit obtained without PEG, the deposit formed in the presence of this additive is very different. The SEM image and EDS analysis for this coating are showed in Figure 9.

This figure shows that the deposit formed is compact and homogeneous with a cauliflower-like morphology; however, once again, the presence of manganese in the deposit could not be detected. The change in the morphology of the deposit may be associated with the partial adsorption of the additive on the electrode surface during the electrodeposition of Zn^{2+} [40]. In addition, the XRD analysis exhibited in Figure 10 revealed that the deposit is comprised principally of Zn crystals in the plane (101), corroborating the EDS results.

Figure 9. SEM image of the deposit formed on AISI 1018 steel electrode at −1.6 V vs. (Ag/AgCl), t = 15 min, from solution S1. The results for the EDS analysis are shown in the inset.
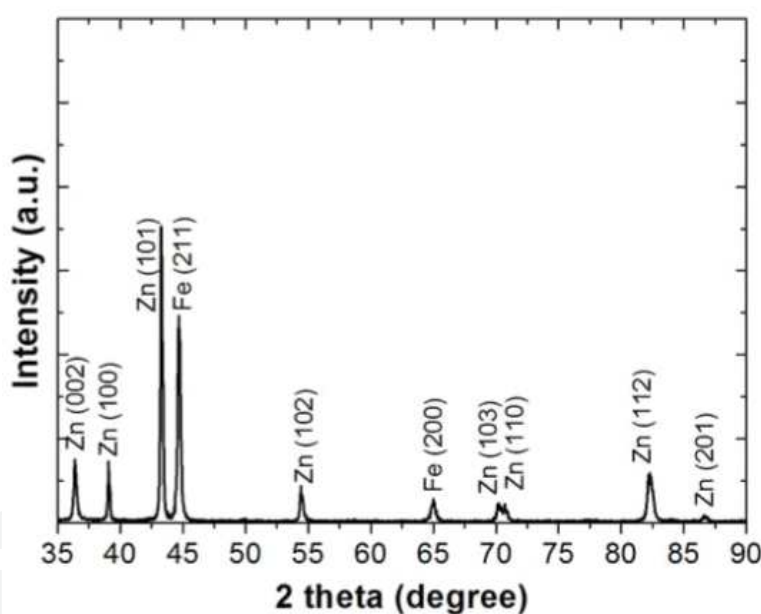
Figure 10. X-ray diffraction (XRD) pattern of the deposit obtained on AISI 1018 steel electrode at −1.6 V vs. (Ag/AgCl), t = 15 min, using the solution S1 (with PEG$_{10,000}$ as additive).

As it was not possible to obtain films containing Zn-Mn alloy through potentiostatic electro-deposition, coatings were obtained by galvanostatic deposition. As the current density stabilized at around -10 mA cm^{-2} with the presence of PEG in the electrolytic bath during potentiostatic electrodeposition at -1.6 V, this current density was chosen for the attempted galvanostatic electrodeposition of the Zn-Mn alloy. Figure 11 shows the chronopotentiometric curves obtained.
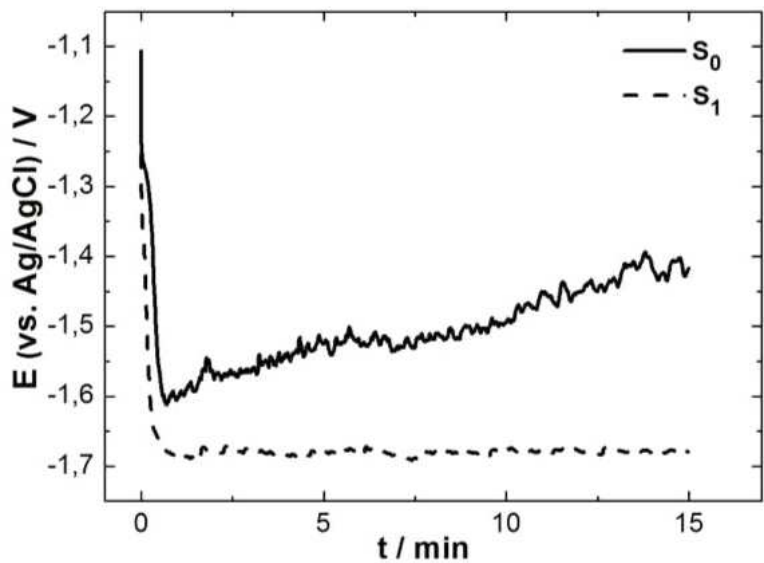
Figure 11. Chronopotentiometric curves obtained during electrodeposition of the deposits on AISI 1018 steel electrode from base solution S0 and solution S1.

In the absence of PEG the potential changed during the electrodeposition, resulting in a rough and irregular deposit, as evidenced in the SEM analysis. On the other hand, when the additive was added to the base solution, the deposition potential stabilized at around -1.68 V at the beginning of the electrodeposition. Additives such as PEG can shift the potential of Zn deposition to more negative values, enabling Zn alloys to be obtained with metals for which the deposition potentials are very negative [30]. In addition, the use of PEG as an additive allowed a compact and homogeneous deposit to be obtained.
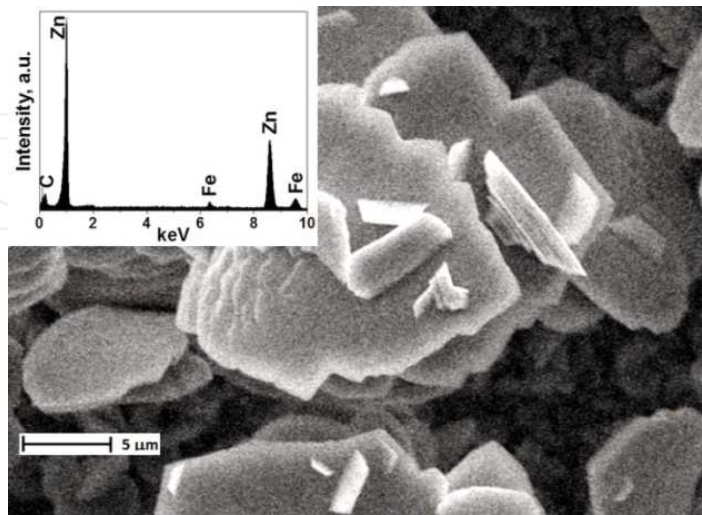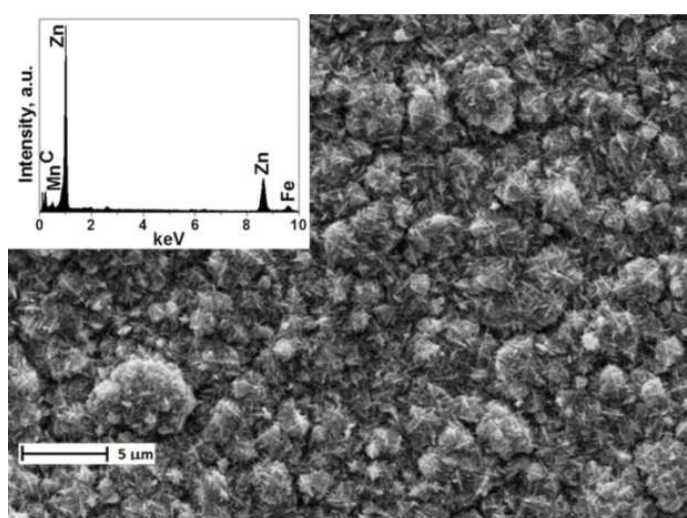

Figure 12. SEM image of the deposit formed on AISI 1018 steel electrode at -10 mA cm^{-2}, t = 15 min, from solution S0. The results for the EDS analysis are shown in the inset.

Figure 12 shows the SEM image of the deposit obtained galvanostatically at -10 mA cm^{-2} in the absence of PEG. The deposit formed is porous and with grains of diverse dimensions irregularly distributed on the substrate surface. The EDS analysis (inset in Figure 12) revealed that there is no manganese present in the coating.

In addition, the XRD patterns of the film showed above were very similar as those obtained during the potentiostatic deposition at -1.2 V from solution S0n (see Figure 6) indicating only the presence of the Zn crystals in different planes.

The results obtained in the presence of PEG indicated the formation of the Zn-Mn alloy during galvanostatic electrodeposition. Figure 13 shows the SEM micrograph of the deposit obtained under these conditions. The results indicate that the PEG decreased the mean size of grains inducing the formation of a smooth deposit. Although the EDS analysis did not clearly indicate the presence of Mn in the deposit.

Figure 13. SEM image of the deposit formed on AISI 1018 steel electrode at −10 mA cm^{-2}, t = 15 min, from solution S1. The results for the EDS analysis are shown in the inset.

The XRD results, exhibited in Figure 14 showed a diffractogram characteristic of a mixture of Zn and ε-phase Zn-Mn with different crystallographic. This finding may be related to the low manganese content, around 2% wt in the deposit. Ballesteros et al.[30] have reported that the presence of additives such as PEG can shift the potential of Zn deposition to very negative values. Such behavior is associated with the partial adsorption of PEG onto the substrate surface. The authors related that in the presence this additive the electrodeposition of zinc can occurs in two different ways. First, the zinc is electrodeposited onto the active sites on the electrode surface that are not blocked by adsorbed PEG molecules. In second, the zinc is electrodeposited onto the active sites that are liberated when PEG molecules are desorbs from electrode surface. This occurs in potential very more negative than the first. The effect of displacement of the zinc reduction potential to more negative values is known as cathodic polarization. Accordingly, potentials as negative as -1.6V vs. SCE could be used to obtain deposits of zinc alloys with metals such as Mn. Similar XRD results were observed by Sylla *et*

al. [32]. They reported a Mn content of 1% wt in a Zn-Mn alloy deposit obtained from a chloride-based acidic bath containing PEG as an additive. The authors postulated that the presence of PEG allowed the formation of a compact and homogeneous deposit with cauliflower-like morphology. However, the presence of PEG in the solution hindered manganese deposition and inhibited the formation of the ζ-phase Zn-Mn. It is important to note that the peaks observed in our study for Zn and the phases of Zn-Mn alloy are very close and some overlap may have occurred.
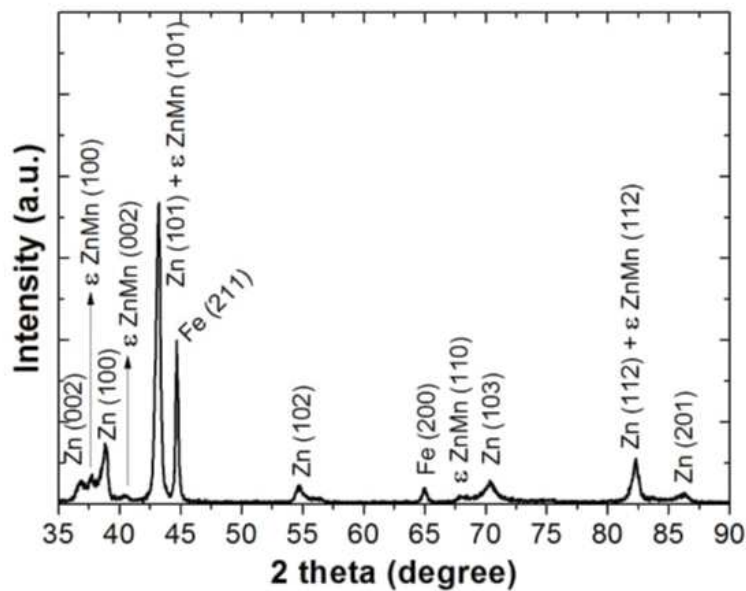

Figure 14. X-ray diffraction (XRD) pattern of a deposit obtained on AISI 1018 steel electrode at -10 mA cm^{-2}, t = 15 min from solution S1 (with PEG$_{10,000}$ as additive)

Table 4 shows a summary of all parameters used in the electrodeposition and some characteristics of the deposits obtained.

Without additive Deposit			
-1.2 V	Homogeneous, comprised by hexagonal plates		only Zn
-1.6 V	Amorphous and porous, Zn and Mn(OH) 2		(~ 8% w/t Mn)
-10 mA cm^{-2}	Amorphous and porous		only Zn
With additive Deposit			
-1.2 V	Homogeneous , comprised by hexagonal crystals		only Zn
-1.6 V	Homogeneous, cauliflower morphology		only Zn
-10 mA cm^{-2}	Homogeneous, smooth		Zn, Zn-Mn alloys, (~2% w/t Mn)

Table 4. Electrodeposition parameters and characteristics of the deposits obtained

The evaluation of the corrosion resistance of the coating obtained could be performed by measurements of polarization curves. Figure 15 shows the polarization curves of the produced coatings in a solution containing NaCl 3% (w/v).
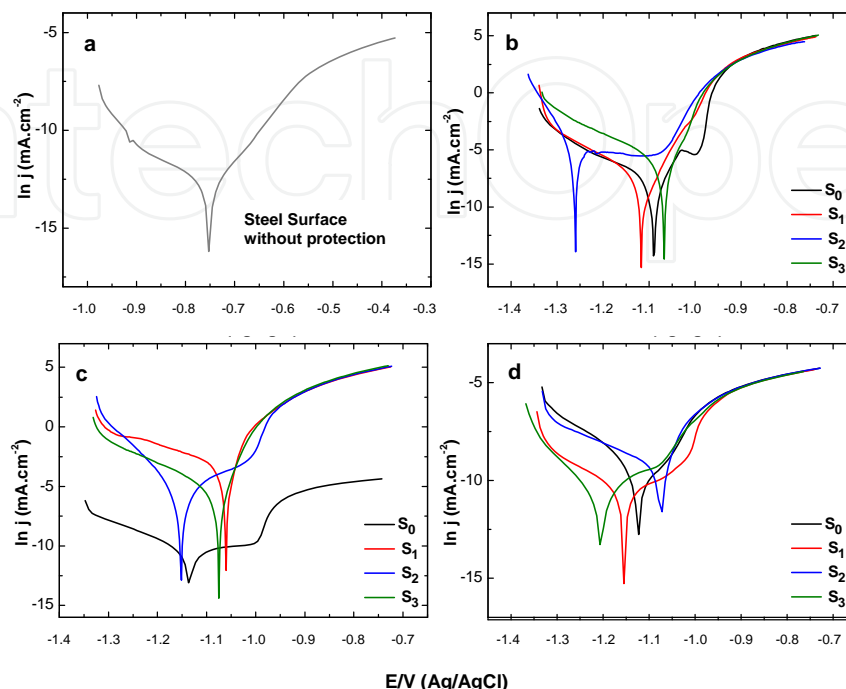
Figure 15. Potentialdynamic Polarization Curves (a) steel surface without protection (b) coating obtained potentiostaticly at -1.2 V vs (Ag/AgCl$_{sat.}$); (c) coating obtained potentiostaticly at -1,6 V vs (Ag/AgCl$_{sat.}$) and (d) coating obtained galvanostaticly at -10mA.cm^{-2}.

The results showed above include the measurements of the coatings obtained using NH$_4$SCN as additive to illustrate the poor protection of the coating produced with this additive due to the lack of homogeneity as described above (see Table 3). The curves showed in Figure 15 indicate that in general, all coatings shift the corrosion potential value (E$_{corr}$) to negative regions when compared with the E$_{corr}$ of the substrate (-0.77 V), this behavior is characteristic for the formation of cathode coatings. It could be also noted from Figure 15 that the corrosion current density (i$_{corr}$) is relatively higher for the coating that presented more negative values of E$_{corr}$. This fact could be seen as divergences but it needs to take in account that the coating that presented more negative values for E$_{corr}$ presented also higher roughness, fact that increase their superficial area causing this increase in current.

Almost at the same time that the work described in this text was done, others experiments using a very similar approach were done by Brito *et al.* [29]. These authors used H$_2$SO$_4$ solution to leaching spent Zn-C and used methylamine as addictive. They found that the quality of deposits produced from lixiviation depends strongly on the magnitude of the electrodeposition current; homogeneous and uniform deposit layers with good anticorrosive properties were obtained, preferentially, at low current densities. The Mn/Zn mass ratios in the produced deposit layers are influenced by electrodeposition currents and the electrodeposition duration.

Lower electrodeposition currents and shorter electrodeposition duration improve the deposition of Mn in relation to Zn. The presence of the methylamine, also benefit the deposition of Mn and that the addition of methylamine to the electrodeposition baths contributes to the establishment of deposit coatings, with better anticorrosive properties.

4. Conclusions

The results reported by our group[28] and by the group of the Portalegre Polytechnical Institute - Portugal[29] demonstrate that it is possible to obtain galvanic coatings in a bath prepared from zinc and manganese recovered from exhausted zinc-carbon batteries. Additionally these showed that the production of a protective Zn-Mn layer over steel related to the substitution of the primary painting process on metallic parts produced in foundries is possible to be developed as practical application.

Specifically thought in the results obtained in the experiments described it could be observed that the presence of polyethylene glycol or methylamine as additives in the electrolytic bath during electrochemical deposition favors the obtainment of a compact and homogeneous deposit containing a mixture of Zn and a Zn-Mn alloy, with a manganese content in the range of 2% to 7% in weight and the electrodeposited coatings with higher Mn content improve the anticorrosiveness of mild steel in saline environments. The proposed method may represent an alternative use for zinc and manganese recovered from exhausted alkaline and zinc-carbon batteries and thus minimize the adverse environment impacts caused by these residues. Moreover lixiviation solutions resulting from the hydrometallurgical treatment of spent domestic batteries, mainly, $Zn–MnO_2$ batteries can be valued directly as electrodeposition baths for zinc and zinc alloys.

The fact that the methodology developed for recycling batteries can now produce the separation of the elements of which these batteries are made can open new avenues of application for these recovered materials. As an example it could be produced nanostructures of Zinc Oxide by electrodeposition over different kind of surfaces that could be used as quantum dots in photovoltaic devices. Also it could be produce magnetic films from the hydrometallurgical treatment of spent $Zn–MnO_2$ batteries by the electrochemical deposition of ferrites with different contents of Zn and Mn in the structure. However these subjects are still possibilities, because no work involving these potentials could be found in the literature.

Acknowledgements

Author details

Paulo S. da Silva[1], Jose M. Maciel[2], Karen Wohnrath[2], Almir Spinelli[1] and Jarem R. Garcia[2*]

1 Chemistry Department, Federal University of Santa Catarina, Florianópolis, SC, Brazil

2 Chemistry Department, State University of Ponta Grossa, Ponta Grossa, PR, Brazil

References

[1] Naseri Joda NRashchi F. Recovery of Ultra-Fine Grained Silver and Copper from PC Board Scraps. Separation and Purification Technology (2012). , 92-36.

[2] Park, Y. J, & Fray, D. J. Recovery of high purity precious metals from printed circuit boards, Journal of Hazardous Materials (2009). , 164-1152.

[3] Hageluken, C. Improving metal returns and eco-efficiency in electronics recycling, in: Proceedings of the 2006 IEEE International Symposium on Electronics and the Environment, San Francisco, USA, (2006). , 218-223.

[4] Cui, J, & Zhang, L. Metallurgical recovery of metals from electronic waste: a review, Journal of Hazardous Materials (2008). , 58-228.

[5] Quinet, P, Proost, J, & Van Lierde, A. Recovery of precious metals from electronic scrap by hydrometallurgical processing routes. Minerals and Metallurgical Processing (2005). , 22(1), 17-22.

[6] Ruffino, B, Zanetti, M. C, & Marini, P. A mechanical pre-treatment process for the valorization of useful fractions from spent batteries. Resources, Conservation and Recycling (2011). , 55-309.

[7] Bernardes, A. M, Espinosa, D. C. R, & Tenório, J. A. S. Collection and recycling of portable batteries: a worldwide overview compared to the Brazilian situation. Journal of Powder Sources (2003). , 124-586.

[8] Salgado, A. L, et al. Recovery of zinc and manganese from spent alkaline batteries by liquid-liquid extraction with Cyanex 272. Journal of Power Sources (2003). , 115-367.

[9] Bernardes, A. M, Espinosa, D. C. R, & Tenório, J. A. S. Recycling of batteries: a review of current processes and technologies. Journal of Powder Sources (2004). , 130-291.

[10] Nougueira, C. A, & Margarido, F. Battery recycling by hydrometallurgy: evaluation of simultaneous treatment of several cell systems. Energy Technology (2012). , 227-234.

[11] Komilis, D, Bandi, D, Kakaronis, G, & Zouppouris, G. The influence of spent household batteries to the organic fraction of municipal solid wastes during composting. Science of the Total Environment. (2011). , 409-2555.

[12] Brenniman, G. R, et al. Automotive and household batteries. In: KREITH, Frank, Handbook of Solid Waste Management, New York: McGraw-Hill. (1994). , 9.

[13] Rydh, C. J, & Svard, B. Impact on global metal flows arising from the use of portable rechargeable batteries. The Science of the Total Environment (2003). , 302-167.

[14] Salgado, A. L, Veloso, A. M. O, Pereira, D. D, Gontijo, G. S, Salum, A, & Mansur, M. B. Recovery of zinc and manganese from spent alkaline batteries by liquid-liquid extraction with Cyanex 272. Journal of Power Sources (2003). , 115-367.

[15] Sayilgan, E, Kukrer, T, Civelekoglu, G, Ferella, F, Akcil, A, Veglio, F, & Kitis, M. A review of technologies for the recovery of metals from spent alkaline and zinc-carbon batteries. Hydrometallurgy (2009). , 97-158.

[16] http://wwwmma.gov.br/port/conama/legiabre.cfm?codlegi=589 (Accessed 30 November (2012).

[17] Provazi, K, Campos, B. A, Espinosa, D. C. R, & Tenório, J. A. S. Metal separation from mixed types of batteries using selective precipitation and liquid-liquid extraction techniques. Waste Management (2011). , 31-59.

[18] Nan, J, et al. Recycling Spent Zinc Manganese Dioxide Batteries Through Synthesizing Zn-Mn Ferrite Magnetic Materials. Journal of Hazardous Materials. (2006). , 133, 257-261.

[19] Rascio, D. C. et. al. Reaproveitamento de Óxidos de Manganês de Pilhas Descartadas para Eletrocatálise da Reação de Redução de Oxigênio em Meio Básico, Química Nova (2010). , 33(3), 730-733.

[20] Veloso, L. R. S, et al. Development of a hydrometallurgical route for the recovery of zinc and manganese from spent alkaline batteries, Journal of Power Sources (2005). , 152-295.

[21] Afonso, J. C. Processamento da Pasta Eletrolítica de Pilhas Usadas, Química Nova (2003). , 26(4), 573-577.

[22] Bocchi, N, Ferracin, L. C, & Biaggio, S. R. Pilhas e Baterias: Funcionamento e Impacto Ambiental. Química Nova na Escola (2000). , 11-3.

[23] Gervais, C, & Ouki, S. K. Effects of foundry dusts on the mechanical, microstructural and leaching characteristics of a cementitious system. Waste Management Series (2000). , 1-782.

[24] Belardia, G, Lavecchiab, R, Medicib, F, & Piga, L. Thermal treatment for recovery of manganese and zinc from zinc-carbon and alkaline spent batteries. Waste Management, (2012). , 32(10), 1945-1951.

[25] Rossi, G. Biohydrometallurgy. McGraw-Hill, Hamburg (1990).

[26] Rohwerder, T, Gehrke, T, Kinzler, K, & Sand, W. Bioleaching review part A: Progress in Bioleaching, fundamentals and mechanisms of bacterial metal sulfide oxidation. Applied Microbiology Biotechnology. (2003). , 63-239.

[27] Xin, B, Jiang, W, Aslam, H, Zhang, K, Liu, C, Wang, R, & Yutao, W. Bioleaching of zinc and manganese from spent Zn-Mn batteries and mechanism exploration. Bioresource technology (2012). , 106-147.

[28] da Silva PS., Schmitz E. P. S., Spinelli A., Garcia J. R. Electrodeposition of Zn and Zn-Mn alloy coatings from an electrolytic bath prepared by recovery of exhausted zinc-carbon batteries. Journal of Power Sources (2012). , 210-116.

[29] Brito, P. S. D, Patrício, S, Rodrigues, L. F, & Sequeira, C. A. C. Electrodeposition of Zn-Mn alloys from recycling Zn-MnO$_2$ batteries solutions. Surface & Coatings Technology (2012). , 206-3036.

[30] Ballesteros, J. C, Díaz-arista, P, Meas, Y, Ortega, R, & Trejo, G. Zinc electrodeposition in the presence of polyethylene glycol 20000 Electrochimica Acta (2007). , 52-3686.

[31] Díaz-arista, P, Ortiz, Z. I, Ruiz, H, Ortega, R, Meas, Y, & Trejo, G. Electrodeposition and characterization of Zn-Mn alloy coatings obtained from a chloride-based acidic bath containing ammonium thiocyanate as an additive. Surface & Coating. Technology (2009). , 203-1167.

[32] Sylla, D, Creus, J, Savall, C, Roggy, O, & Gadouleau, M. Refait Ph. Electrodeposition of Zn-Mn alloys on steel from acidic Zn-Mn chloride solutions. Thin Solid Films (2003).

[33] Savall, C, Rebere, C, Sylla, D, & Gadouleau, M. Refait Ph., Creus J. Morphological and structural characterisation of electrodeposited Zn-Mn alloys from acidic chloride bath. Material Science & Engeneering (2006). A 430 165.

[34] Bucko, M, Rogan, J, Stevanovi, S. I, Peri-gruji, A, & Bajat, J. B. Initial corrosion protection of Zn-Mn alloys electrodeposited from alkaline solution. Corrosion Science (2011). , 53-2861.

[35] Ortiz, Z. I, Díaz-arista, P, Meas, Y, Ortega-borges, R, & Trejo, G. Characterization of the corrosion products of electrodeposited Zn, Zn-Co and Zn-Mn alloys coatings. Corrosion Science (2009). , 51-2703.

[36] Gomes, A. da Silva Pereira M.I. Pulsed electrodeposition of Zn in the presence of surfactants. Electrochimica Acta (2006). , 51-1342.

[37] Song, K. D, Kim, K. B, Han, S. H, & Lee, H. Effect of additives on hydrogen evolution and absorption during Zn electrodeposition investigated by EQCM. Electrochemistry & Solid-State Letter (2004). CC24., 20.

[38] Díaz-arista, P, Antano-lópez, R, Meas, Y, Ortega, R, Chainet, E, Ozil, P, & Trejo, G. EQCM study of the electrodeposition of manganese in the presence of ammonium thiocyanate in chloride-based acidic solutions. Electrochimica Acta (2006).

[39] Atlas of Eh-pH diagramsIntercomparison of Thermodynamic Geological Survey of Japan Open File Report National of Advanced Industrial Science and Technology, May (2005). www.gsj.jp/GDB/openfile/files/no0419/openfile419e.pdf.Accessed 2012. (419)

[40] Kim, J. W, Lee, J. Y, & Park, S. M. Effects of Organic Additives on Zinc Electrodeposition at Iron Electrodes Studied by EQCM and in Situ STM. Langmuir (2004). , 20-459.